

A Novel Red Fluorescent Protein Orthotopic Pancreatic Cancer Model for the Preclinical Evaluation of Chemotherapeutics

Matthew H. Katz, M.D.,* Shinako Takimoto, B.S.,* Daniel Spivack, M.D.,* A. R. Moossa, M.D.,* Robert M. Hoffman, Ph.D.,*† and Michael Bouvet, M.D.*¹

*Department of Surgery, University of California at San Diego, San Diego, California; and †AntiCancer, Inc., San Diego, California

Submitted for publication April 18, 2003

Background. Realistic models of pancreatic cancer are necessary to develop effective drugs for the disease. More aggressive tumor models enhanced by brighter fluorescent biomarkers to follow the disease in real time would enhance the ability to predict accurately the effect of novel therapeutics on this particularly malignant human cancer.

Materials and methods. A novel, highly fluorescent, red fluorescent protein (RFP)-expressing pancreatic cancer model was orthotopically established in nude mice. The MIA-PaCa-2 human pancreatic cancer cell line was transduced with RFP and grown subcutaneously. Fluorescent tumor fragments were then surgically transplanted onto the nude mouse pancreas. Groups treated with intraperitoneal gemcitabine or intravenous irinotecan were sequentially imaged to compare, in real time, the antimetastatic and antitumor effects of these agents compared with untreated controls.

Results. Rapid tumor growth and widespread metastases developed in untreated mice within 2 weeks, leading to a median survival of 21 days. In contrast, significant tumor growth suppression and consequent increase in survival (32.5 days, $P = 0.009$) were achieved with CPT-11. Gemcitabine highly improved survival (72 days, $P = 0.004$) by inducing transient tumor regression over the first 3 weeks. However, at this time, growth and dissemination occurred despite continued treatment, suggesting the development of tumor resistance. The antimetastatic efficacy of each

drug was followed noninvasively in real time by imaging the RFP-expressing tumor and metastases, and was confirmed by fluorescent open imaging of autopsy specimens.

Conclusions. This highly metastatic model reliably simulates the aggressive course of human pancreatic cancer. Noninvasive, sequential imaging permits quantification of tumor growth and dissemination and, thereby, real time evaluation of therapeutic efficacy. These features make this model an ideal, preclinical system with which to study novel therapeutics for pancreatic cancer. © 2003 Elsevier Inc. All rights reserved.

Key Words: pancreatic cancer; red fluorescent protein; gemcitabine; irinotecan; orthotopic mouse model.

INTRODUCTION

The use of orthotopic animal models of pancreatic cancer in the preclinical evaluation of novel antitumor therapeutics is well described. In orthotopic models of pancreatic cancer, injected human cancer cell suspensions [1] or surgically transplanted human tumor fragments [2] are grown directly on the organ. These xenografts grow in their native milieu, may cause locoregional growth and spontaneous distant metastases, which maintain relative genetic stability during growth and dissemination [3]. Because of this, they are more accurate cancer models than subcutaneous xenografts, which typically do not metastasize [4] and may respond differently to chemotherapeutic agents than *in situ* human disease [5]. By accurately modeling human disease, orthotopic xenograft models may be used to develop and test novel therapeutics, and predict their activity on human pancreatic cancer.

We have previously described the use of the green fluorescent protein (GFP), cloned from the biolumines-

This study was supported in part by the Department of Health Services, California Cancer Research Program (Grant 97-120B), and US National Cancer Institute Grants P30 CA 23100-1851 and R43-89779.

¹ To whom correspondence and reprint requests should be addressed at Department of Surgery, University of California, San Diego, 3350 La Jolla Village Drive (112E), San Diego, CA 92161. E-mail: mbouvet@ucsd.edu.



cent jellyfish *Aequorea Victoria*, to engineer fluorescent human cancer xenografts [6–11]. In these models, the GFP gene is stably transduced into human cancer cell lines, which subsequently express GFP at high levels *in vitro* and *in vivo*, including primary and metastatic tumor deposits. We have described this technology to engineer green fluorescent orthotopic models of pancreatic cancer [6–8], as well as lung cancer [9], prostate cancer [10], breast cancer [11], and others. Using these GFP models, the sequential, real-time imaging of tumor growth and dissemination is possible in the live animal without the use of anesthesia, contrast agents, laparotomy, or invasive procedures. In preclinical trials of novel therapeutic agents, this feature can be exploited and used to monitor, evaluate, and compare the effects of different agents on tumor growth and spread using simple light boxes and imaging equipment.

In this study, we show the use of a novel, highly metastatic, orthotopic mouse model of pancreatic cancer that uses the MIA-PaCa-2 pancreatic cancer cell line. MIA-PaCa-2 is engineered to express stably high levels of the *Discosoma species* coral red fluorescent protein (RFP) [12]. RFP is a new fluorescent biomarker that possesses enhanced optical qualities that enable it to be used instead of, or as an adjunct to, GFP-based systems. Orthotopic implantation of highly red-fluorescent human pancreatic tumor fragments onto the pancreas spontaneously yields extensive, locoregional, primary tumor growth and the development of distant metastases. The primary and metastatic tumors can be visualized, tracked, and imaged, in real time, using selective tumor RFP fluorescence. Treatment with two well-described therapeutic agents, gemcitabine and CPT-11, is used to show the ability to compare therapeutic efficacy among drugs using this unique preclinical model.

MATERIALS AND METHODS

Cell Line

The MIA-PaCa-2 pancreatic cancer cell line was obtained from the American Type Culture Collection (Rockville, MD). Cells were maintained in Dulbecco modified Eagle medium (DMEM) supplemented with 10% heat-inactivated fetal bovine serum, and 1% penicillin and streptomycin (Gibco-BRL, Life Technologies, Inc., Grand Island, NY). Cells were kept incubated at 37°C in a 5% CO₂ incubator.

RFP Retroviral Transduction and Selection of MIA-PaCa-2-RFP Pancreatic Cancer Cells

The pDsRed-2 vector (Clontech Laboratories Inc., Palo Alto, CA) was used to engineer MIA-PaCa-2 clones stably expressing RFP. This vector expresses RFP and the neomycin resistance gene on the same bicistronic message. The pDsRed-2 retrovirus was produced in PT67 packaging cells. RFP transduction was initiated by incubating 20% confluent MIA-PaCa-2 cells with retroviral supernatants of the packaging cells and DMEM for 24 h. Fresh medium was replenished

at this time, and cells were allowed to grow in the absence of retrovirus for 12 h. This procedure was repeated until high levels of RFP expression, as determined using fluorescence microscopy, were achieved. Cells were then harvested by trypsin/ethylenediaminetetraacetic acid (EDTA) and subcultured into selective medium that contained 200 µg/ml of G418 (Geneticin, Invitrogen Corp., Carlsbad, CA). The level of G418 was increased to 2,000 µg/ml stepwise. Clones expressing high levels of RFP were isolated with cloning cylinders as needed, and were amplified and transferred using conventional culture methods. High RFP-expression clones were isolated in the absence of G418 for 10 passages to select for stable expression of RFP *in vivo*.

Cell Viability Assay

MIA-PaCa-2 and MIA-PaCa-2-RFP cells were distributed into 96 well plates at a density of 2,000 cells per well. The number of viable cells was subsequently determined using CellTiter 96 Aqueous One Solution Cell Proliferation assay (Promega Corp., Madison, WI) at 24, 48, 72, 96, and 120-h time points. Briefly, at each time point, 20 µl CellTiter 96 solution was added to each well. The plates were then incubated for 1 h, after which the absorbance of each well was read at a wavelength of 490 nm. All assays were performed in quadruplicate, and each assay was repeated at least twice.

Animals

Male nude mice (NCR-nu) between 4 and 6 weeks of age were maintained in a barrier facility on High Efficiency Particulate Air (HEPA)-filtered racks. The animals were fed with autoclaved laboratory rodent diet (Teckland LM-485; Western Research Products, Orange, CA). Animal experiments were performed in accordance with the Guidelines for the Care and Use of Laboratory Animals (National Institutes of Health Publication Number 85-23) under National Institutes of Health assurance number A3873-01.

Subcutaneous Tumor Growth

MIA-PaCa-2-RFP cells were harvested by trypsinization and washed 3 times with phosphate-buffered saline. Cells were injected subcutaneously into study mice in a total volume of 0.2 ml within 30 min of harvesting. The subcutaneous tumors were used as the source of tissue for orthotopic implantation of tissue onto the pancreas.

Surgical Orthotopic Implantation of MIA-PaCa-2-RFP Tumors

Orthotopic, red-fluorescent human pancreatic cancer xenografts were established in nude mice with surgical orthotopic implantation (SOI) [2]. Briefly, MIA-PaCa-2-RFP tumors in the exponential growth phase, grown subcutaneously in nude mice, were resected aseptically. Necrotic tissues were cut away, and the remaining healthy tumor tissues were cut with scissors and minced into 1 mm³ pieces in Roswell Park Memorial Institute (RPMI) 1640 medium. Mice were then anesthetized, and their abdomens were sterilized with alcohol. An incision was created through the left upper abdominal pararectal line and peritoneum. The pancreas was carefully exposed, and 2 tumor pieces were transplanted onto the middle of the gland using a single 8-0 surgical suture (Davis-Geck, Inc., Manati, Puerto Rico). The pancreas was then returned into the peritoneal cavity, and the abdominal wall and the skin were closed in 2 layers using 6-0 surgical suture. All procedures were performed with a 7× microscope (Olympus America, Inc., Melville, NY) or standard surgical loupes.

In Vivo Dosing of Gemcitabine and CPT-11

Ten days after surgical orthotopic implantation of MIA-PaCa-2-RFP tumors, mice were randomized into 3 groups of 10 mice each.

The first group served as a negative control and did not receive treatment. Mice in group 2 were treated every 3 days with intravenous injections of irinotecan (CPT-11, Camptosar, Pharmacia & Upjohn Co., Kalamazoo, MI) via the dorsal tail vein at a dose of 40 mg/kg/dose [13]. Mice in the third group received twice weekly intraperitoneal injections of gemcitabine (Gemzar, Eli Lilly, Indianapolis, IN), at 150 mg/kg/dose [14]. Dosing was performed on the aforementioned schedules until death.

External *In Vivo* Whole Body Imaging

Twice weekly, whole-body images of each mouse were obtained by placing the mouse in a fluorescent light box equipped with a fiber-optic light source of 470 nm (Lighttools Research, Encinitas, CA). Emitted fluorescence was collected through a long-pass filter GG475 (Chroma Technology, Battleboro, VT) on a Hamamatsu C5810 3-chip cooled color CCD camera (Hamamatsu Photonics Systems, Bridgewater, NJ). High resolution images of 1024×724 pixels were captured directly on an IBM personal computer (IBM, White Plains, NY) and analyzed using Image Pro Plus 3.1 software (Media Cybernetics, Silver Spring, MD). At each imaging time point, the real-time determination of tumor burden was performed by quantifying fluorescent surface area, as described previously [6].

Internal Imaging, Analysis of Metastasis, and Correlation of Open and Closed Measurements of Tumor Burden

Mice were killed and explored when they appeared pre-morbid. After anesthesia, postmortem external fluorescent images were obtained. Then each mouse underwent laparotomy and median sternotomy. RFP expression was visualized in the light box described above, facilitating identification of primary and metastatic pancreatic tumor. After performing full-body, open images, the solid organs were removed and were thoroughly examined for any evidence of metastasis using a Leica fluorescence stereo microscope model LZ12 (Leica Microsystems, Inc., Bannockburn, IL) equipped with a mercury 50-W lamp power supply. Selective excitation of RFP was produced through a D425/60 band-pass filter and 470 DCXR dichroic mirror. Emitted fluorescence was collected on the Hamamatsu camera system described above.

To confirm a correlation between tumor burdens, as determined by externally visualized RFP fluorescence, and standard measurements of tumor volume, the primary tumor of each mouse was used. Primary tumor volume was first calculated using the formula (long diameter \times short diameter²)/2, where long diameter and short diameter measurements were precisely obtained in the open animal. The externally-visualized RFP fluorescent area was then determined as described above. The correlation coefficient r could then be calculated between tumor volume and RFP fluorescence.

Histologic Analysis

The primary orthotopic tumors were removed and saved for histologic analysis performed with standard hematoxylin and eosin (H & E) staining.

Statistical Analysis

Differences among treatment groups were assessed using analysis of variance (ANOVA) and Student t test using Statistica software (Statsoft, Inc., Tulsa, OK). Kaplan-Meier analysis with a log-rank test was used to determine survival and differences between treatment groups. Correlation was measured using Pearson product moment correlation coefficient; $P \leq 0.05$ was statistically significant.

RESULTS

In Vitro MIA-PaCa-2 and MIA-PaCa-2-RFP Isolation and Growth

The pDsRed-2 retroviral-vector transduced cells were able to grow *in vitro* at levels of G418 up to 2,000 $\mu\text{g/ml}$. The selected G418-resistant pancreatic cancer cells had bright RFP fluorescence that remained stable in the absence of selective medium after numerous passages (Fig. 1A). Cell proliferation rates of the parental cells and the RFP transductants were determined to be statistically equivalent by 5-day cell proliferation assay (data not shown).

Survival

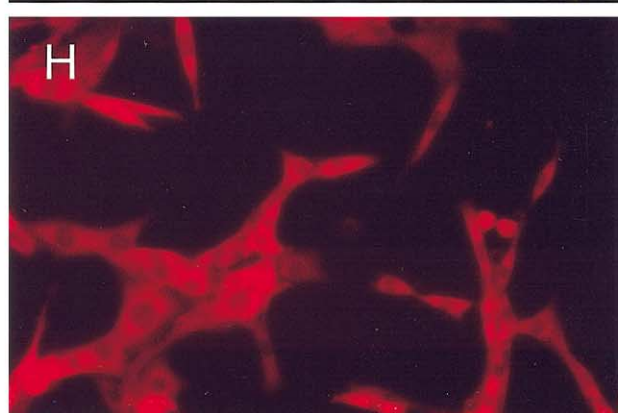
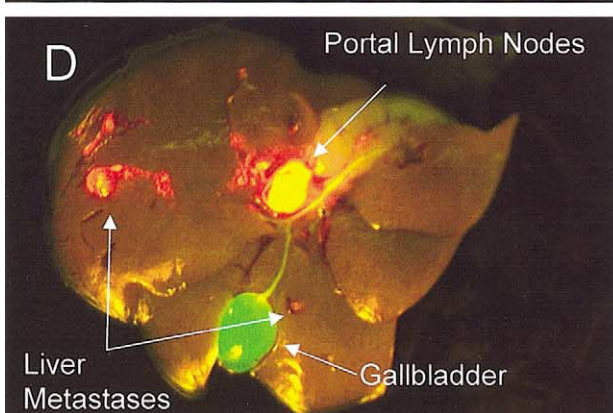
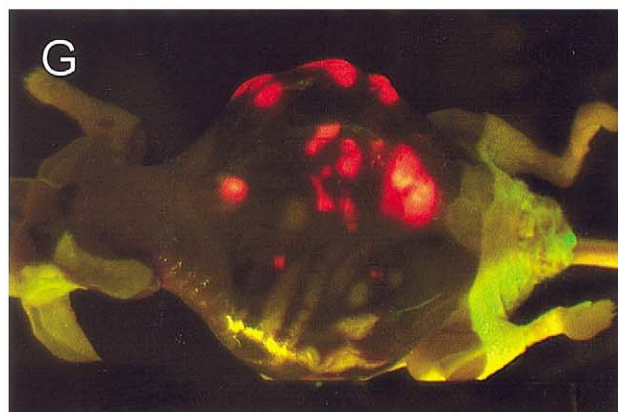
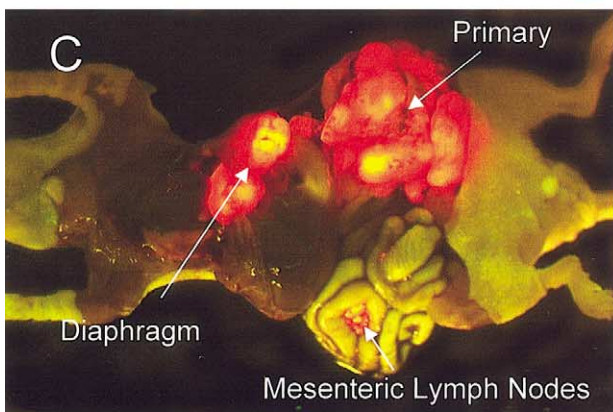
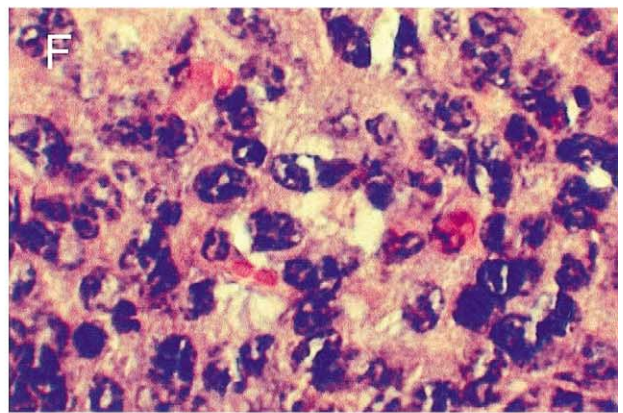
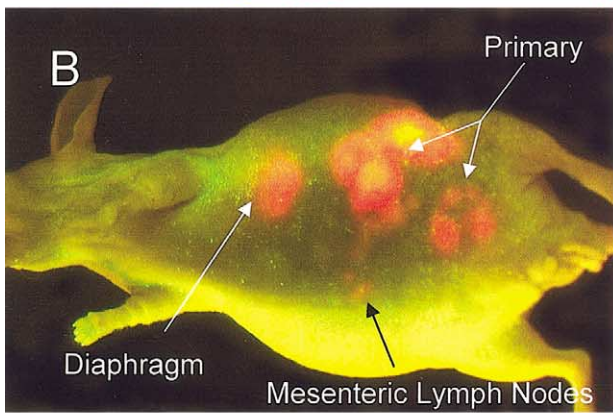
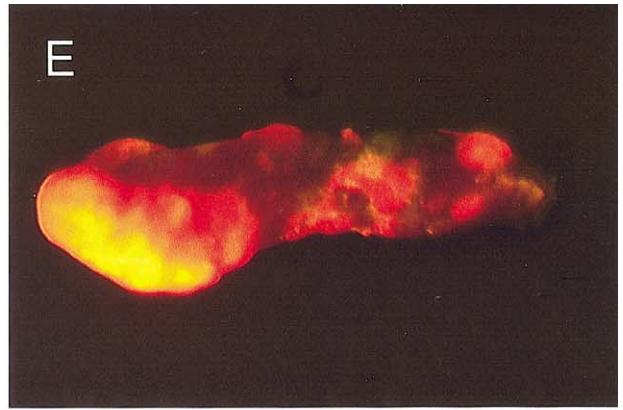
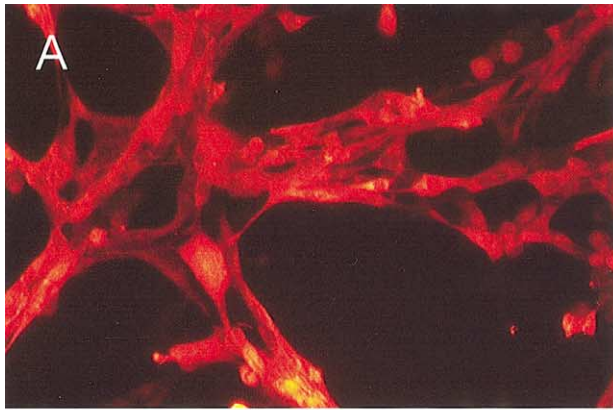
Death from disease was rapid in untreated mice, which had a median survival of 21 days. Administration of CPT-11 and gemcitabine significantly prolonged survival compared with control, increasing the median survival to 32.5 ($P = 0.009$) and 72 days ($P = 0.004$), respectively (Fig. 2). Mice treated with gemcitabine had a survival advantage compared with those treated with CPT-11 ($P = 0.003$).

Real-Time Visualization of Tumor Growth and Metastasis, and Quantification of Therapeutic Efficacy

Tumor RFP fluorescence enabled real-time, sequential whole-body imaging (Fig. 3) and quantification of tumor burden (Fig. 4) without the need for anesthesia, laparotomy, contrast agents, or invasive procedures. The visualized area of red fluorescence emitted by the internally implanted tumors correlated strongly with tumor volume ($r = 0.89$, $P < 0.05$), as calculated using standard measurements obtained at autopsy (Fig. 5). The correlation was stronger for animals that did not exhibit ascites (0.95, $P < 0.05$) than those that did retain intra-abdominal fluid (0.83, $P < 0.05$).

In control animals, rapid primary tumor growth over the first 2 weeks was accompanied by progressive intra-abdominal tumor dissemination to all 4 abdominal quadrants. Seventy percent of the animals had visually disseminated disease by day 17. In contrast, treated mice had slower rates of tumor growth. At day 17, 80% of CPT-11-treated mice had only localized disease. These mice had, on average, approximately half the visualized, total tumor burden as control animals (Fig. 4A). Progression of disease in this group was rapid over the third and fourth weeks, leading ultimately to death from disease in all animals.

The growth-suppressive effects of gemcitabine were dramatically visualized by whole-body imaging (Fig. 3). A total of 80% of mice in the gemcitabine group had visible primary tumor on day 10 after SOI, at which time treatment was initiated (Fig. 4C). Subsequent treatment with gemcitabine not only prevented the



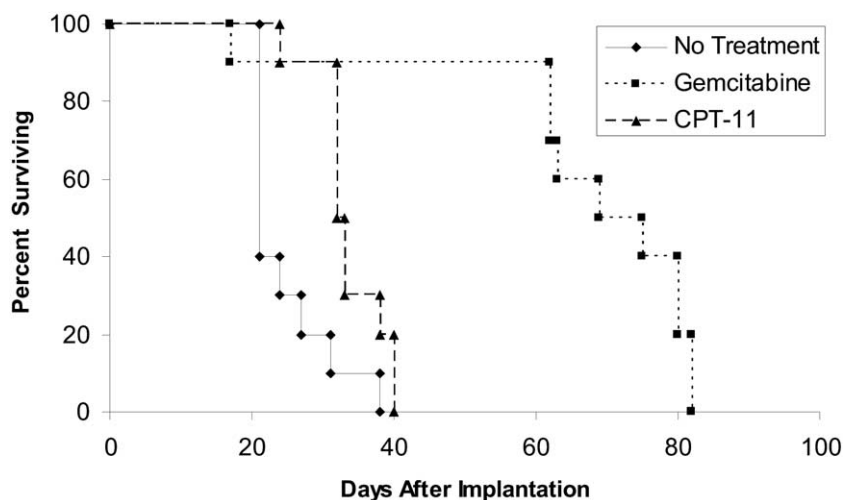


FIG. 2. Treatment with gemcitabine and CPT-11 significantly prolonged survival in mice with MIA-PaCa-2-RFP pancreatic tumors. Treatment was initiated 10 days after surgical orthotopic implantation (SOI) and continued until death using the dosage schedules described in the Materials and Methods. Median survival was increased from 21 days in the control group to 32.5 days in mice treated with CPT-11 ($P = 0.009$) and 72 days in mice treated with gemcitabine ($P = 0.004$). \blacklozenge , control; \blacktriangle , CPT-11; \blacksquare , gemcitabine.

rapid development of metastases but also induced regression of the primary tumor (*i.e.*, 50% of mice had visible tumor on day 13, while 20% had evident tumor on day 17). Calculation of tumor burden using quantification of RFP fluorescence (Figs. 4A and B) showed that the total tumor burden in these mice did not return to the level seen on day 10 until approximately day 36, after which progressive growth and distant metastasis accelerated despite continued treatment. Progression of disease in each group, as visualized by real-time, RFP fluorescence imaging, had a strong inverse correlation with survival.

Patterns of Growth and Metastasis Determined at Autopsy

Untreated, orthotopically transplanted MIA-PaCa-2-RFP tumors rapidly produced extensive locoregional and disseminated disease (Figs. 1B-E). At autopsy, all control mice showed metastatic disease in the periportal and intestinal lymph nodes, spleen, and retroperitoneum. Intra-abdominal ascites (80%), peritoneal carcinomatosis (80%), and metastasis to the diaphragm (80%) and liver (40%) were also common (Fig. 6). Tumors had histologic features consistent with poorly

differentiated pancreatic carcinoma visualized with routine H & E staining (Fig. 1F). Ascites fluid drawn and cultured at autopsy yielded high RFP-expressing clones of MIA-PaCa-2-RFP cells (Figs. 1G and H).

Gemcitabine and CPT-11 had an antimetastatic effect on the SOI-implanted MIA-PaCa-2-RFP tumors. Treatment with gemcitabine reduced the frequency of metastases to the diaphragm by 50%, portal lymph nodes 70%, liver 30%, and intestinal lymph nodes 50%, compared with controls. CPT-11 appeared to have less of a dramatic effect, although a definite reduction in carcinomatosis and metastases to the portal lymph nodes and liver was shown after treatment with this agent (Fig. 6).

DISCUSSION

Human pancreatic cancer typically leads to death from disease in less than 2 years [15, 16]. Tumor propensity for locoregional spread and distant metastasis, an ability to remain asymptomatic in its early stages, and a predilection for tumor recurrence after therapy all contribute to the grim prognosis that is faced by patients with this disease. Therapeutic options for

FIG. 1. (A) High level expression of red fluorescent protein (RFP) in MIA-PaCa-2 cells *in vitro*. Cells were transfected with pDsRed-2 vector and selected for stable expression of RFP in increasing concentrations of G418 (original magnification $\times 400$). (B) External and (C) open images of a single, representative, control mouse at autopsy on day 17 after surgical orthotopic implantation (SOI). Extensive locoregional and metastatic growth is visualized by selectively exciting RFP. A strong correlation between the fluorescence visualized externally and that obtained after laparotomy is evident, despite the presence of intra-abdominal ascites. (D) The liver, (E) spleen, and other solid organs were removed at autopsy and examined for evidence of metastatic disease. (F) Excised tumors showed morphology consistent with poorly differentiated pancreatic cancer visualized with hematoxylin and eosin (H & E) staining (original magnification $\times 100$). (G) Transperitoneal view of a second representative control mouse, with skin removed at the time of sacrifice, showing a large amount of intra-abdominal ascites. (H) Colonies of MIA-PaCa-2-RFP clones were easily retrieved and cultured from this aspirated ascites fluid (original magnification $\times 400$).

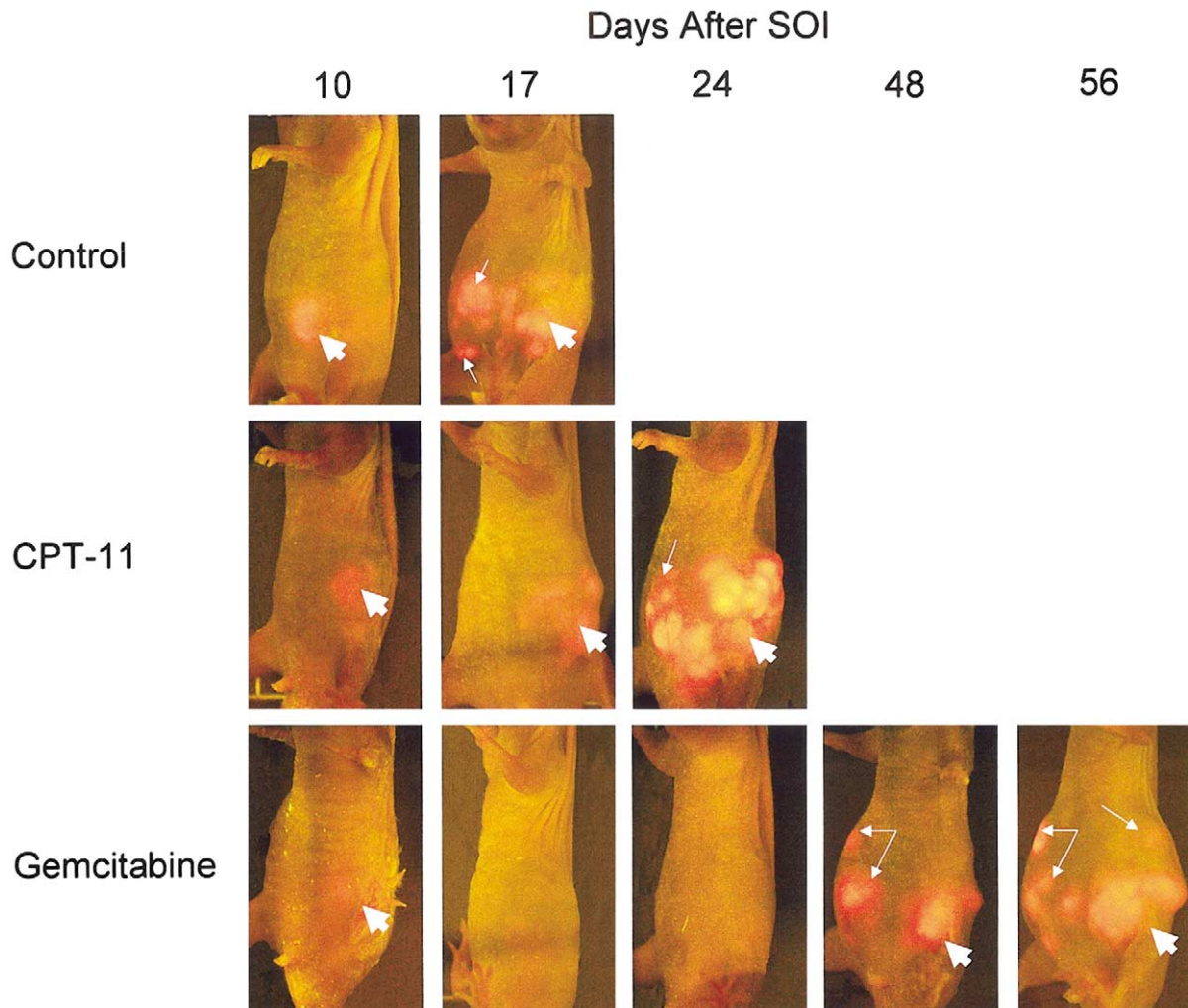


FIG. 3. Real-time, *in vivo* imaging of MIA-PaCa-2-RFP pancreatic cancer progression and evaluation of therapeutic efficacy over time. Representative mice from each treatment group on days 10, 17, 24, 48, and 56 after tumor implantation are shown. Thick arrows show primary tumor, and thin arrows indicate metastatic tumor. CPT-11 suppressed primary and metastatic tumor growth compared with controls. In contrast, gemcitabine successfully induced temporary regression of disease over the first month, after which growth and distant metastasis of tumor accelerated despite continued treatment.

these patients remain limited. Presently, complete surgical tumor resection with pancreaticoduodenectomy, combined with adjuvant chemotherapy and radiation in select patients, offers the only chance for a permanent cure.

Traditionally, treatment of pancreatic cancer has used multimodality therapy, including the chemotherapeutic agent 5-FU, despite inconsistent data regarding its efficacy [17, 18]. Over the last decade, the anti-metabolite gemcitabine has been an effective antitumor agent against pancreatic cancer and has an advantage over 5-FU in this regard [19]. The drug has now become the accepted treatment of advanced disease [19, 20]. The adjuvant use of gemcitabine may also improve survival, as shown in our laboratory using a green fluorescent, orthotopic mouse model [21], but these data have not been confirmed in a large, random-

ized human trial. The topoisomerase inhibitor CPT-11 has also been tested alone [22] and as part of a combination therapy with gemcitabine [23], but data do not yet exist to support its routine use.

Novel therapeutic strategies are urgently needed for pancreatic cancer. To facilitate the discovery and evaluation of new chemotherapeutics, we have designed this red fluorescent, orthotopic pancreatic cancer model. Like previous models we have designed, this model uses selective tumor fluorescence to facilitate the imaging and tracking of tumor growth and development in real time, in the live animal. However, this model differs from our previous models in several important respects. First, this model fluoresces more brightly than the previous pancreatic cancer models we have engineered that involve selective tumor expression of GFP [7]. In addition, red fluorescence is more

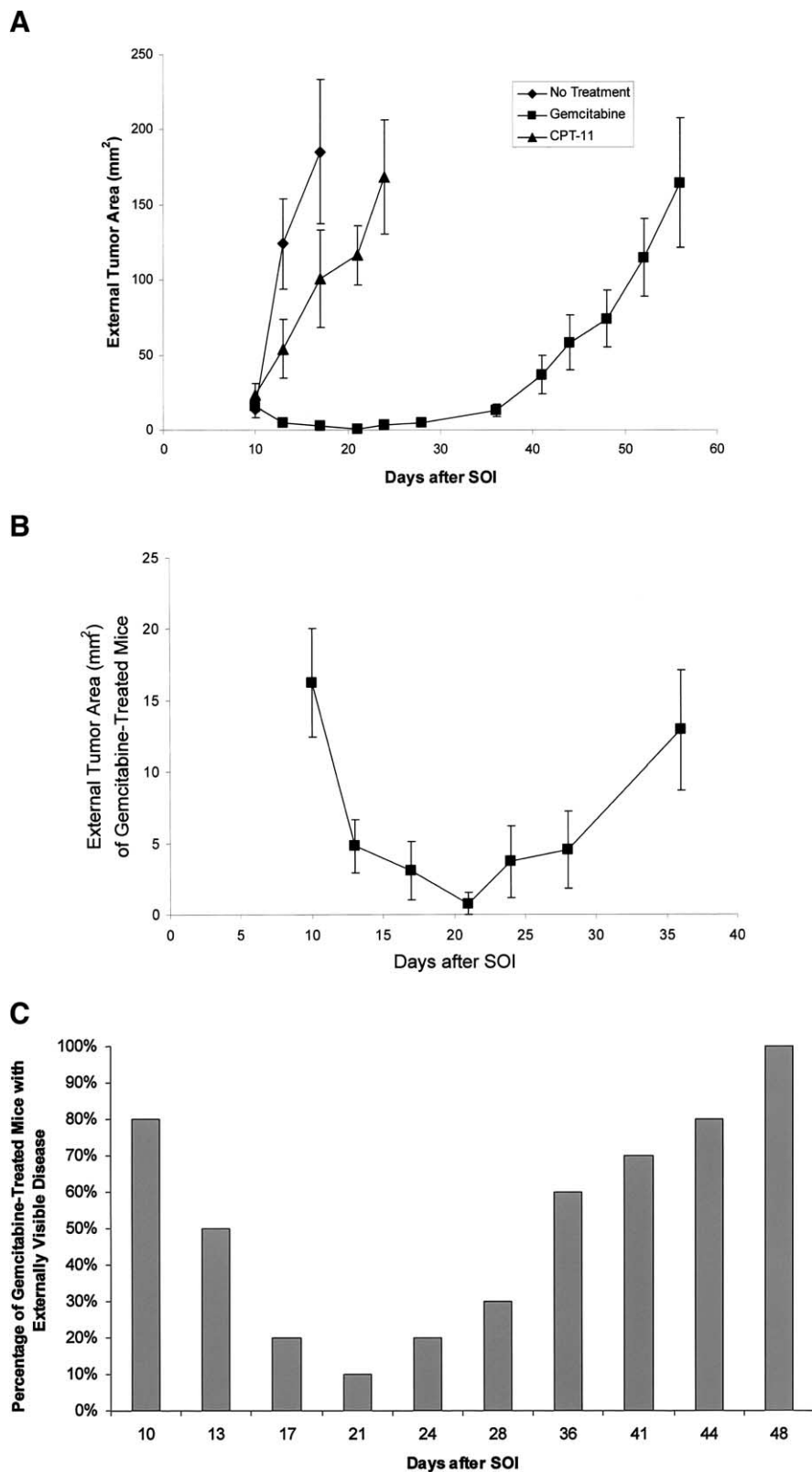


FIG. 4. (A) Gemcitabine and CPT-11 inhibited MIA-PaCa-2-RFP pancreatic cancer growth. Quantification of tumor red fluorescent protein (RFP) fluorescence enabled real-time determination and comparison of tumor load during the course of each treatment. Progression of disease had a strong inverse correlation to survival. Drug treatment was initiated 10 days after surgical orthotopic implantation (SOI) and continued until death using the dosing schedules described in the Materials and Methods. Values represent the mean area of external fluorescence \pm standard error (SE) for live animals in each treatment group ($P < 0.05$ for each time point). \blacklozenge , control; \blacktriangle , CPT-11; \blacksquare , gemcitabine. (B) Tumor size in the gemcitabine-treated group during the first 40 days of treatment. Early, transient tumor regression was achieved by the intraperitoneal delivery of gemcitabine. (C) The percentage of gemcitabine-treated mice with visible tumor transiently decreased as tumor regression was achieved with this agent. Over time, these mice re-accumulated externally visible disease despite continued treatment.

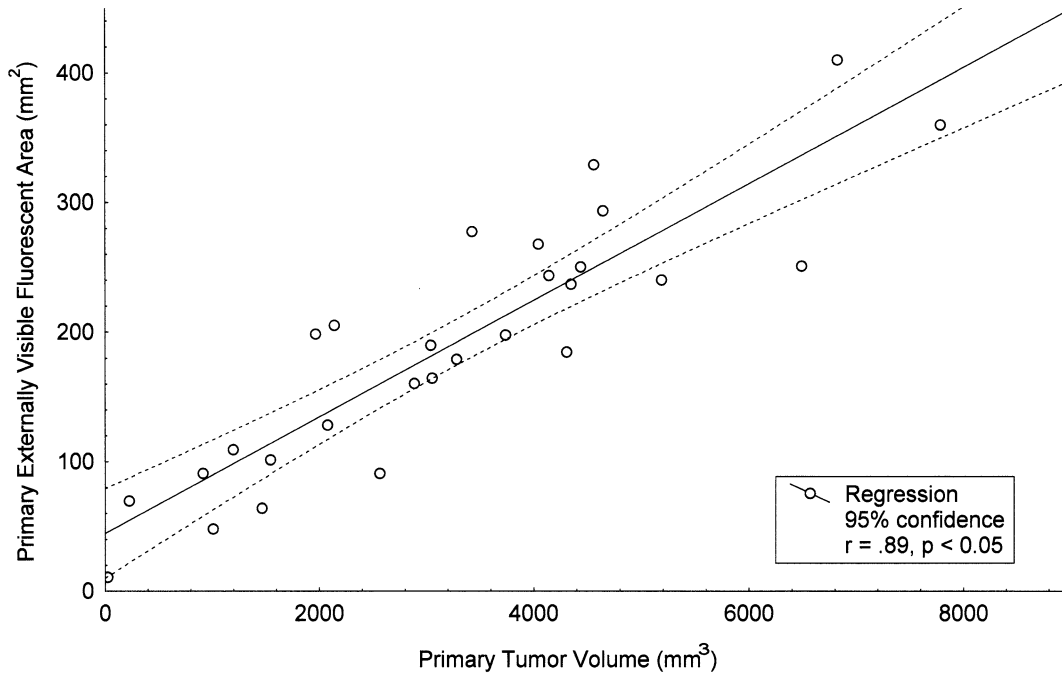


FIG. 5. Red fluorescent area quantified using external fluorescence imaging correlated strongly with tumor volume measured directly. At autopsy, measurement of externally visualized fluorescent area and direct measurements of the primary tumor of each mouse were obtained, as described in the Materials and Methods. Significant correlation ($r = 0.89, P < 0.05$) was observed between these values. As expected, the correlation was less, though still strongly significant, in mice with intra-abdominal ascites ($r = 0.83, P < 0.05$) compared with those without ascites ($r = 0.95, P < 0.05$).

tumor-specific than green. This is because mouse skin and hair, as well as urine and bile, may all fluoresce green under fluorescent light (see Fig. 1D). Therefore, the optical qualities of this system enable a more reliable acquisition of images of small tumor deposits without the need for skin flaps or other manipulations

[24]. Serial, high contrast images of pancreatic primary and metastatic tumors are attainable through the skin, without the need for animal anesthesia, contrast, or invasive procedures, all of which increase animal morbidity and experimental variability.

We have previously shown that the external optical

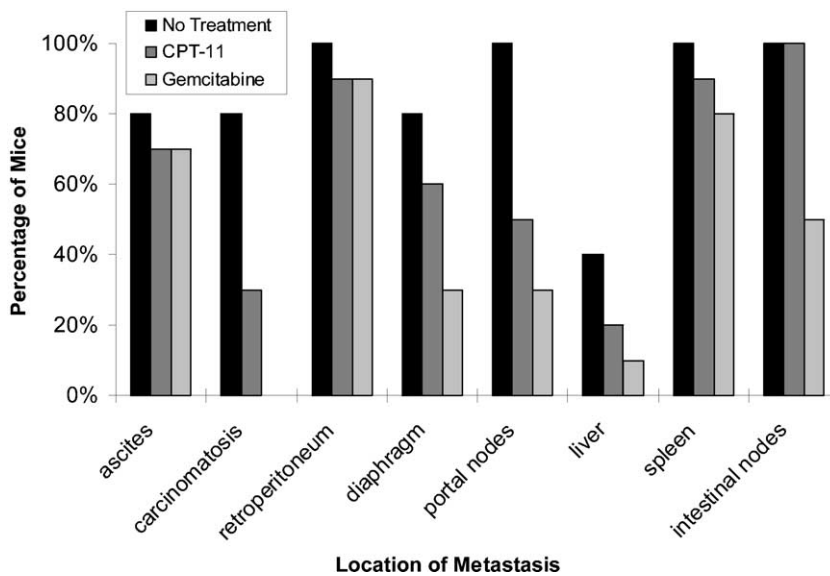


FIG. 6. Treatment of MIA-PaCa-2-RFP pancreatic cancer with gemcitabine and CPT-11 had varying effects on metastatic tumor growth. Percentage of mice in each treatment group with metastasis in the specified location at autopsy is shown.

images acquired using our green fluorescent models correlate well with direct intravital images performed under more invasive conditions [6]. In this study, we have confirmed a strong correlation between externally visualized red fluorescence and calculated tumor volume. Therefore, serial calculations of fluorescent area can be used, as we have here, to compare the antitumor effects of different therapeutics over time. As expected, the correlation is not perfect. We have identified ascites as one factor that may reduce the sensitivity of our fluorescent imaging system. This effect may occur due to an increase in light scattering secondary to an increase in the distance between the internally growing tumor and the skin, or to an interposition of blood, cells, and debris. Similarly, anatomic considerations, such as overlying loops of bowel between tumor and skin, can reduce fluorescence visualization on the skin surface. Nonetheless, as in our previous systems, we have clearly shown that measured externally visualized fluorescence may serve as a reliable surrogate for volume data that can only be made under more invasive conditions.

The present model is also notable for the aggressive nature of the MIA-PaCa-2-RFP tumor, which rapidly and spontaneously leads to peritoneal, lymphatic, and solid organ metastases, as well as ascites, in a large proportion of untreated animals. This is in marked contrast to even our prior models, which required 2 to 3 months before locoregional and distant metastatic tumor growth was significant enough to cause death. Human pancreatic cancer is a particularly aggressive tumor that often escapes early diagnosis. Therefore, approximately 50% of patients have advanced disease at diagnosis. Moreover, tumor recurrence after maximal treatment, to solid organs and the peritoneum, is routine [25]. This model reliably leads to a clinically relevant pattern of advanced disease spontaneously, without the need for portal vein [26] or intraperitoneal inoculation of cell suspensions [27], which may bypass important steps of the metastatic cascade [28].

The present model facilitates sequential optical imaging of tumor growth and metastasis. It rapidly and reliably produces spontaneous distant metastases. Moreover, despite its extremely aggressive nature, it responds favorably to therapeutics with known activity against human disease. These features make it an ideal model to develop and evaluate the effects of novel therapeutics on pancreatic cancer.

REFERENCES

- Schwarz, R. E., McCarty, T. M., Peralta, E. A., Diamond, D. J., and Ellenhorn, J. D. An orthotopic in vivo model of human pancreatic cancer. *Surgery* **126**: 562, 1999.
- Fu, X., Guadagni, F., and Hoffman, R. M. A metastatic nude-mouse model of human pancreatic cancer constructed orthotopically with histologically intact patient specimens. *Proc. Natl. Acad. Sci. U.S.A.* **89**: 5645, 1992.
- Reyes, G., Villanueva, A., Garcia, C., Sancho, F. J., Piulats, J., Lluis, F., and Capella, G. Orthotopic xenografts of human pancreatic carcinomas acquire genetic aberrations during dissemination in nude mice. *Cancer Res.* **56**: 5713, 1996.
- Kyriazis, A. P., DiPersio, L., Michael, G. J., Pesce, A. J., and Stinnett, J. D. Growth patterns and metastatic behavior of human tumors growing in athymic mice. *Cancer Res.* **38**: 3186, 1978.
- Kuo, T. H., Kubota, T., Watanabe, M., Furukawa, T., Kase, S., Tanino, H., Saikawa, Y., Ishibiki, K., Kitajima, M., and Hoffman, R. M. Site-specific chemosensitivity of human small-cell lung carcinoma growing orthotopically compared to subcutaneously in SCID mice: The importance of orthotopic models to obtain relevant drug evaluation data. *Anticancer Res.* **13**: 627, 1993.
- Bouvet, M., Wang, J., Nardin, S. R., Nassirpour, R., Yang, M., Baranov, E., Jiang, P., Moossa, A. R., and Hoffman, R. M. Real-time optical imaging of primary tumor growth and multiple metastatic events in a pancreatic cancer orthotopic model. *Cancer Res.* **62**: 1534, 2002.
- Bouvet, M., Yang, M., Nardin, S., Wang, X., Jiang, P., Baranov, E., Moossa, A. R., and Hoffman, R. M. Chronologically-specific metastatic targeting of human pancreatic tumors in orthotopic models. *Clin. Exp. Metastasis* **18**: 213, 2000.
- Sun, F. X., Tohgo, A., Bouvet, M., Yagi, S., Nassirpour, R., Moossa, A. R., and Hoffman, R. M. Efficacy of camptothecin analog DX-8951f (Exatecan Mesylate) on human pancreatic cancer in an orthotopic metastatic model. *Cancer Res.* **63**: 80, 2003.
- Rashidi, B., Yang, M., Jiang, P., Baranov, E., An, Z., Wang, X., Moossa, A. R., and Hoffman, R. M. A highly metastatic Lewis lung carcinoma orthotopic green fluorescent protein model. *Clin. Exp. Metastasis* **18**: 57, 2000.
- Yang, M., Jiang, P., Sun, F. X., Hasegawa, S., Baranov, E., Chishima, T., Shimada, H., Moossa, A. R., and Hoffman, R. M. A fluorescent orthotopic bone metastasis model of human prostate cancer. *Cancer Res.* **59**: 781, 1999.
- Yang, M., Baranov, E., Li, X. M., Wang, J. W., Jiang, P., Li, L., Moossa, A. R., Penman, S., and Hoffman, R. M. Whole-body and intravital optical imaging of angiogenesis in orthotopically implanted tumors. *Proc. Natl. Acad. Sci. U.S.A.* **98**: 2616, 2001.
- Matz, M. V., Fradkov, A. F., Labas, Y. A., Savitsky, A. P., Zaraisky, A. G., Markelov, M. L., and Lukyanov, S. A. Fluorescent proteins from nonbioluminescent Anthozoa species. *Nat. Biotechnol.* **17**: 969, 1999.
- Stewart, C. F., Zamboni, W. C., Crom, W. R., and Houghton, P. J. Disposition of irinotecan and SN-38 following oral and intravenous irinotecan dosing in mice. *Cancer Chemother. Pharmacol.* **40**: 259, 1997.
- Braakhuis, B. J., Ruiz van Haperen, V. W., Boven, E., Veerman, G., and Peters, G. J. Schedule-dependent antitumor effect of gemcitabine in in vivo model system. *Semin. Oncol.* **22**: 42, 1995.
- Bouvet, M., Gamagami, R. A., Gilpin, E. A., Romeo, O., Sasson, A., Easter, D. W., and Moossa, A. R. Factors influencing survival after resection for periampullary neoplasms. *Am. J. Surg.* **180**: 13, 2000.
- Yeo, C. J., Cameron, J. L., Sohn, T. A., Lillemoe, K. D., Pitt, H. A., Talamini, M. A., Hruban, R. H., Ord, S. E., Sauter, P. K., Coleman, J., Zahurak, M. L., Grochow, L. B., and Abrams, R. A. Six hundred fifty consecutive pancreaticoduodenectomies in the 1990s: Pathology, complications, and outcomes. *Ann. Surg.* **226**: 248, 1997.
- Klinkenbijn, J. H., Jeekel, J., Sahmoud, T., van Pel, R., Couvreur, M. L., Veenhof, C. H., Arnaud, J. P., Gonzalez, D. G.,

- de Wit, L. T., Hennipman, A., and Wils, J. Adjuvant radiotherapy and 5-fluorouracil after curative resection of cancer of the pancreas and periampullary region: Phase III trial of the EORTC gastrointestinal tract cancer cooperative group. *Ann. Surg.* **230**: 776, 1999.
18. Kalsner, M. H., and Ellenberg, S. S. Pancreatic cancer. Adjuvant combined radiation and chemotherapy following curative resection. *Arch. Surg.* **120**: 899, 1985.
19. Burris, H. A. III, Moore, M. J., Andersen, J., Green, M. R., Rothenberg, M. L., Modiano, M. R., Cripps, M. C., Portenoy, R. K., Storniolo, A. M., Tarassoff, P., Nelson, R., Dorr, F. A., Stephens, C. D., and Von Hoff, D. D. Improvements in survival and clinical benefit with gemcitabine as first-line therapy for patients with advanced pancreas cancer: A randomized trial. *J. Clin. Oncol.* **15**: 2403, 1997.
20. Carmichael, J., Fink, U., Russell, R. C., Spittle, M. F., Harris, A. L., Spiessi, G., and Blatter, J. Phase II study of gemcitabine in patients with advanced pancreatic cancer. *Br. J. Cancer* **73**: 101, 1996.
21. Lee, N. C., Bouvet, M., Nardin, S., Jiang, P., Baranov, E., Rashidi, B., Yang, M., Wang, X., Moossa, A. R., and Hoffman, R. M. Antimetastatic efficacy of adjuvant gemcitabine in a pancreatic cancer orthotopic model. *Clin. Exp. Metastasis* **18**: 379, 2000.
22. Wagener, D. J., Verdonk, H. E., Dirix, L. Y., Catimel, G., Siegenthaler, P., Buitenhuis, M., Mathieu-Boue, A., and Verweij, J. Phase II trial of CPT-11 in patients with advanced pancreatic cancer, an EORTC early clinical trials group study. *Ann. Oncol.* **6**: 129, 1995.
23. Stathopoulos, G. P., Rigatos, S. K., Dimopoulos, M. A., Giannakakis, T., Foutzilias, G., Kouroussis, C., Janninis, D., Aravantinos, G., Androulakis, N., Agelaki, S., Stathopoulos, J. G., and Georgoulas, V. Treatment of pancreatic cancer with a combination of irinotecan (CPT-11) and gemcitabine: A multicenter phase II study by the Greek Cooperative Group for Pancreatic Cancer. *Ann. Oncol.* **14**: 388, 2003.
24. Yang, M., Baranov, E., Wang, J. W., Jiang, P., Wang, X., Sun, F. X., Bouvet, M., Moossa, A. R., Penman, S., and Hoffman, R. M. Direct external imaging of nascent cancer, tumor progression, angiogenesis, and metastasis on internal organs in the fluorescent orthotopic model. *Proc. Natl. Acad. Sci. U.S.A.* **99**: 3824, 2002.
25. Johnstone, P. A., and Sindelar, W. F. Patterns of disease recurrence following definitive therapy of adenocarcinoma of the pancreas using surgery and adjuvant radiotherapy: correlations of a clinical trial. *Int. J. Radiat. Oncol. Biol. Phys.* **27**: 831, 1993.
26. Stapfer, M., Hu, J., Wei, D., Groshen, S., and Beart, R. W. Jr. Establishment of a nude mouse model of hepatic metastasis for evaluation of targeted retroviral gene delivery. *J. Surg. Oncol.* **82**: 121, 2003.
27. Nishimori, H., Yasoshima, T., Denno, R., Shishido, T., Hata, F., Honma, T., Ura, H., Yamaguchi, K., Yagihashi, A., Tanaka, H., Kawaguchi, S., Kamiguchi, K., Isomura, H., Sato, N., and Hirata, K. A new peritoneal dissemination model established from the human pancreatic cancer cell line. *Pancreas* **22**: 348, 2001.
28. Alves, F., Contag, S., Missbach, M., Kaspereit, J., Nebendahl, K., Borchers, U., Heidrich, B., Streich, R., and Hiddemann, W. An orthotopic model of ductal adenocarcinoma of the pancreas in severe combined immunodeficient mice representing all steps of the metastatic cascade. *Pancreas* **23**: 227, 2001.